JVSTA Journal of Vacuum Science & Technology A

Atomic layer deposition of Al2O3 for single electron transistors utilizing Pt oxidation and reduction

Michael S. McConnell, Louisa C. Schneider, Golnaz Karbasian, Sergei Rouvimov, Alexei O. Orlov, and Gregory L. Snider

Citation: Journal of Vacuum Science & Technology A **34**, 01A139 (2016); doi: 10.1116/1.4937992
View online: http://dx.doi.org/10.1116/1.4937992
View Table of Contents: http://scitation.aip.org/content/avs/journal/jvsta/34/1?ver=pdfcov
Published by the AVS: Science & Technology of Materials, Interfaces, and Processing

Atomic layer deposition of Al_2O_3 for single electron transistors utilizing Pt oxidation and reduction

Michael S. McConnell,[a] Louisa C. Schneider, Golnaz Karbasian, Sergei Rouvimov, Alexei O. Orlov, and Gregory L. Snider
Department of Electrical Engineering, University of Notre Dame, 275 Fitzpatrick Hall, Notre Dame, Indiana 46556

(Received 5 September 2015; accepted 3 December 2015; published 21 December 2015)

This work describes the fabrication of single electron transistors using electron beam lithography and atomic layer deposition to form nanoscale tunnel transparent junctions of alumina (Al_2O_3) on platinum nanowires using either water or ozone as the oxygen precursor and trimethylaluminum as the aluminum precursor. Using room temperature, low frequency conductance measurements between the source and drain, it was found that devices fabricated using water had higher conductance than devices fabricated with ozone. Subsequent annealing caused both water- and ozone-based devices to increase in conductance by more than 2 orders of magnitude. Furthermore, comparison of devices at low temperatures (~4 K) showed that annealed devices displayed much closer to the ideal behavior (i.e., constant differential conductance) outside of the Coulomb blockade region and that untreated devices showed nonlinear behavior outside of the Coulomb blockade region (i.e., an increase in differential conductance with source-drain voltage bias). Transmission electron microscopy cross-sectional images showed that annealing did not significantly change device geometry, but energy dispersive x-ray spectroscopy showed an unusually large amount of oxygen in the bottom platinum layer. This suggests that the atomic layer deposition process results in the formation of a thin platinum surface oxide, which either decomposes or is reduced during the anneal step, resulting in a tunnel barrier without the in-series native oxide contribution. Furthermore, the difference between ozone- and water-based devices suggests that ozone promotes atomic layer deposition nucleation by oxidizing the surface but that water relies on physisorption of the precursors. To test this theory, devices were exposed to forming gas at room temperature, which also reduces platinum oxide, and a decrease in resistance was observed, as expected. © *2015 American Vacuum Society*. [http://dx.doi.org/10.1116/1.4937992]

I. INTRODUCTION

Single electron transistors (SETs) are like other transistors in that they are three terminal devices with a source, a drain, and a gate used to modulate current, but they also have an "island," which is a conducting region connected to the source and drain by tunnel barriers and capacitively coupled to the gate. The charging energy, which is the energy needed to add a single electron to the island, is given by

$$E_C = \frac{e^2}{2C_\Sigma}, \tag{1}$$

where E_C is the charging energy, e is the elementary charge, and C_Σ is the total capacitance of the island.[1] At low temperatures ($kT \ll E_C$, where k is the Boltzmann constant), electrons do not have enough energy to tunnel to the island, and this is known as Coulomb blockade. The gate voltage V_g (not used in these experiments) can modulate the potential of the island by capacitive coupling. These changes in island potential can take the SET in and out of blockade by increasing or decreasing the energy electrons need to tunnel to the island, resulting in periodic oscillations of conductance in V_g known as Coulomb oscillations.

The second important requirement of SET operation is the source-to-drain conductance G_{ds}, which must satisfy the condition

$$G_{ds} < \frac{e^2}{h} \approx 39\,\mu\text{S}, \tag{2}$$

to prevent quantum fluctuations of electron charge, leading to the delocalization of electrons.[1]

Metal-insulator-metal (MIM) devices are one class of SETs where the source, drain, and island are all composed of a metal (as opposed to a semiconductor) and separated by thin dielectric layers. The most popular MIM SET fabrication technique has been the Dolan bridge,[2] which achieves a small capacitance by using two evaporations through a lithographic mask at different angles and *in situ* oxidation to create a dielectric barrier of native metal oxide between the two metal layers. While using the native oxide of the electrodes has the advantage of simplicity, this technique has poor control over junction formation and can only be used with a limited set of metals (e.g., Al, Cr, and Nb).[1] For this reason, additional fabrication techniques have been sought to achieve high quality dielectrics without dependence upon the native oxide of the source and drain. This work demonstrates that the precise thickness control available through atomic layer deposition (ALD) is advantageous for SET

[a]Electronic mail: mmcconn5@nd.edu

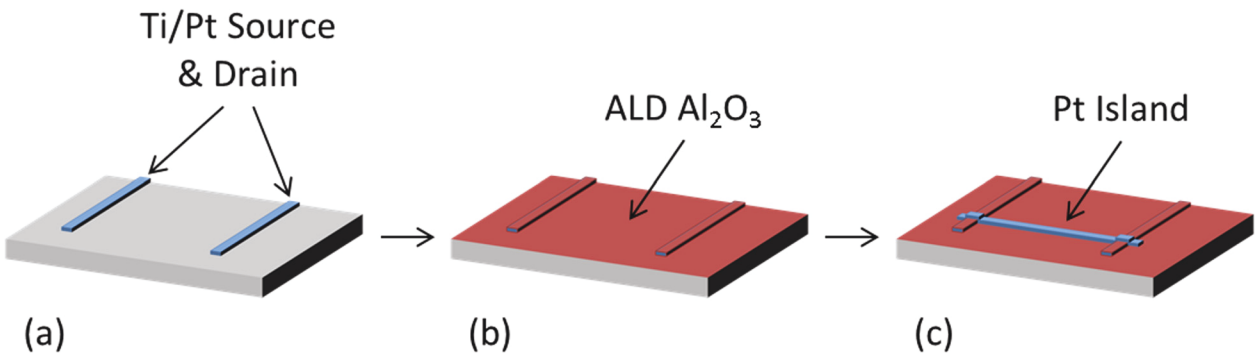

FIG. 1. (Color online) Fabrication process of single electron transistors: (a) the Ti/Pt source and drain are deposited using EBL and liftoff, (b) the sample is coated with 9 cycles of Al_2O_3 using ALD, and (c) the Pt island is formed by EBL and liftoff (gate not shown).

fabrication, and that even with relatively inert metals such as platinum, the native oxide still plays a role in the tunnel barrier.

II. EXPERIMENT

All devices were fabricated on silicon wafers with 500 nm of thermally grown SiO_2 on top (Fig. 1). Electron beam lithography (EBL) was used with liftoff to pattern the source and drain (~60 nm wide) out of evaporated Pt on a Ti adhesion layer (25 and 5 nm thick, respectively, with base pressure $<1 \times 10^{-6}$ Torr). Next, 9 cycles of Al_2O_3 (~1 nm) were deposited at 200 °C in a Cambridge Nanotech Savannah ALD system using either H_2O or O_3 (45 ms pulse), and trimethylaluminum (45 ms pulse) with a 5 s purge time between each step. The growth rate observed, as shown in the transmission electron microscopy (TEM) images, is approximately 1.1 nm/cycle, which agrees well with the growth rates recorded in literature for Al_2O_3 grown on Pt (Ref. 3) but is generally higher than that reported for deposition on hydrogen-passivated Si.[4] Nine cycles were selected as that number consistently provided a measurable conductance that also satisfied Eq. (2). The carrier gas was nitrogen, and the pressure was held at 200 mTorr. Finally, a second EBL step with liftoff was used to pattern the island (~60 nm wide) out of a 30-nm thick layer of evaporated Pt.

Two methods of reducing or decomposing the platinum oxide were investigated: annealing and reduction by forming gas. Annealing was performed in a rapid thermal annealing system at 375 °C in an Ar environment for 3 min with 1 min nitrogen purges before and after the annealing process. In the second method, the sample was held at 32 °C in forming gas (5% H_2 in Ar) for 1 h.

TEM and energy dispersive x-ray spectroscopy (EDX) data were taken using an FEI Titan TEM system. The EDX spectrum was corrected for background signal, and the atomic percentages were calculated using the FEI TITAN software.

III. RESULTS AND DISCUSSION

Devices fabricated with water as the oxidative species in the ALD process showed a strikingly different conductance than devices fabricated with ozone for the same number of cycles. In general, as prepared water-based devices were approximately 3 orders of magnitude more conductive than ozone-based devices, with water-based devices typically having a conductance of ~9 μS while ozone-based devices had a conductance of ~2 nS. Furthermore, across multiple devices fabricated on the same chip, water-based devices showed a much larger spread in conductance than ozone-based devices, as can be seen in Fig. 2.

Both types of devices showed a large increase in conductance of more than 2 orders of magnitude when they were annealed in Ar at 375 °C for 3 min. This was a desirable result for ozone-based devices, resulting in conductances of about 5 μS, but resulted in short-circuited tunnel junctions for water-based devices (~1 mS, which is approximately the conductance of the metal nanowires without a tunnel barrier present). Looking at the standard deviation in conductance for each type of device also illustrates how annealing changes them. The spread in conductance for ozone-based devices is almost unchanged by annealing while the spread decreases noticeably for the water-based devices since the conductance is now limited by the resistance of the source and drain wires instead of the tunnel barriers.

At $kT \ll E_C$, an ideal MIM SET would show constant differential conductance G_{ds} as a function of source–drain bias V_{ds} outside the region of Coulomb blockade (i.e., where

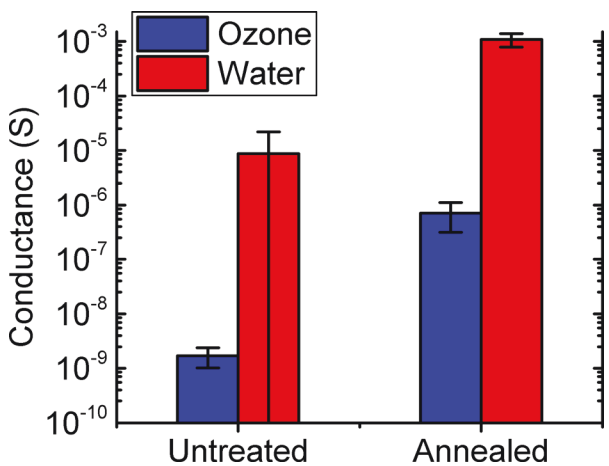

FIG. 2. (Color online) Average conductance and standard deviation over at least 20 devices before and after annealing at 375 °C in Ar for 3 min.

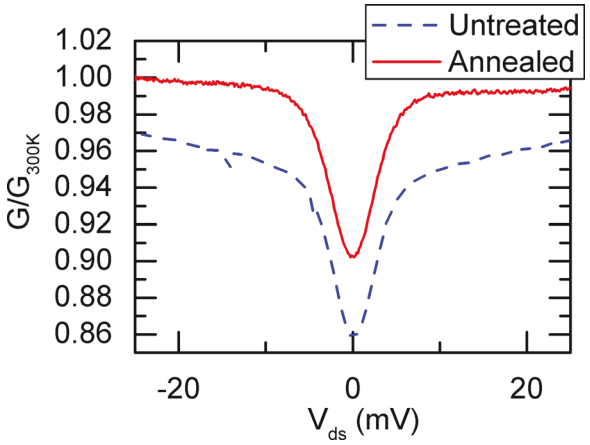

FIG. 3. (Color online) Differential conductance at T = 5 K of an ozone-based device as a function of source–drain voltage before and after anneal normalized by room temperature conductance ($G_{300\ K} = 5$ nS for the untreated device, $G_{300\ K} = 733$ nS for the annealed device). The dip at $V_{ds} = 0$ mV is the Coulomb blockade and the width of this dip is proportional to the charging energy. Outside of the blockaded region, the untreated device shows more nonlinear behavior than the annealed device, which shows nearly constant differential conductance.

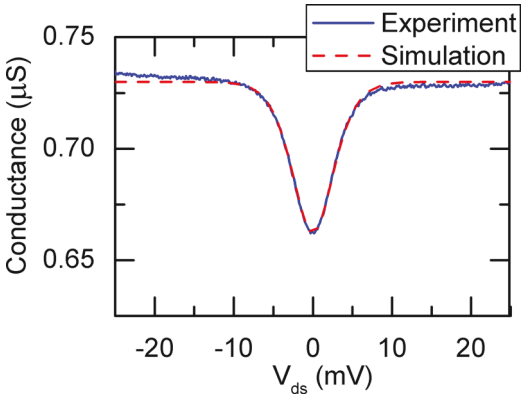

FIG. 4. (Color online) Differential conductance of an annealed, ozone-based device compared to a simulation using the master equation for SETs (Ref. 5).

$V_{ds} \gg E_C/e$). But low temperature testing (T ~ 5 K) of untreated devices showed a strong nonlinear behavior outside of the Coulomb blockade region as can be seen by G_{ds} increasing as a function of V_{ds} in Fig. 3. However, this nonlinear behavior was significantly less noticeable in annealed devices as can be seen in comparison to simulations (Figs. 3 and 4). Also of interest, the width of the Coulomb blockade region in V_{ds}, which is proportional to the charging energy, did not change noticeably with annealing. A near constant charging energy means that the capacitances of the junctions were not noticeably changed by the anneal.

In order to determine the cause of these observations, TEM cross-sectional images of the H_2O-grown ALD tunnel junctions before and after annealing (Fig. 5) were taken. Structurally, both untreated and annealed junctions appeared very similar. However, EDX revealed that the bottom platinum layer near the Pt/Al_2O_3 interface had a higher oxygen content than the platinum of the top interface, as can be seen in Table I and, more significantly, that the oxygen content in the same position was much lower in the annealed sample (Table II). This suggests that during the ALD process, a thin platinum surface oxide is formed on the bottom platinum layer.

While Pt is considered a noble metal without a surface oxide under most conditions, it has been well established in the literature that Pt has at least three different phases of oxide and that a surface oxide can form under the right conditions.[6,7] Given that O_3 is a highly reactive oxidizing agent, the higher resistance of ozone-based devices is likely caused by the oxidation of the platinum surface. Moreover, the most common platinum oxide, PtO_2, is unstable compared to other metal oxides.[6] It dissociates around 500 °C at 1 atm of oxygen partial pressure and lower oxygen partial pressures reduce the decomposition temperature further as can be seen in the Ellingham diagram[8] of Fig. 7.

These characteristics of PtO_2 explain why annealing greatly increased the conductance of ozone-based devices without changing the charging energy. PtO_2 was formed on the bottom layer during the ALD process due to the O_3, but exposure to the high temperature and low oxygen partial pressure (since oxygen was displaced by argon) caused the PtO_2 to dissociate. This dissociation eliminated the resistive PtO_2 layer and increased the conductance. The insignificant change in charging energy can be explained by the fact that

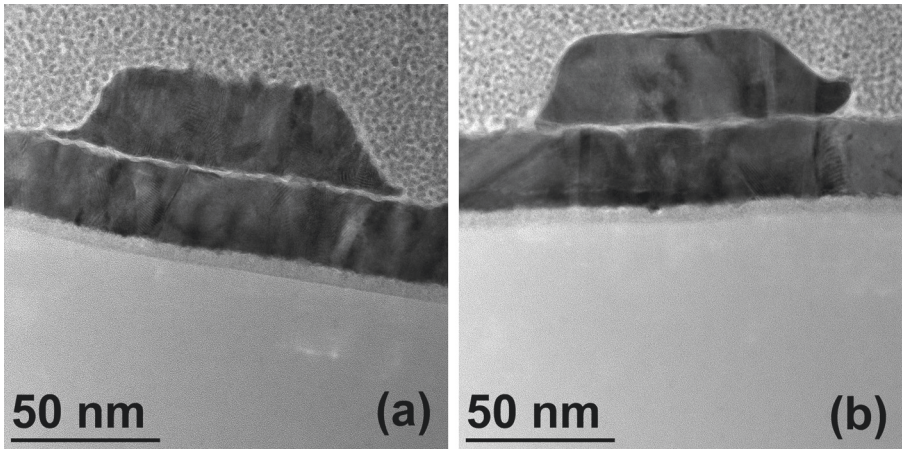

FIG. 5. TEM image of water-based Al_2O_3 tunnel junction (a) before and (b) after annealing.

TABLE I. Atomic percentages before anneal at the numbered positions shown in Fig. 6. Notice that position 2 shows an almost ideal Al/O ratio and also that position 1 in the bottom Pt layer shows a larger amount of O than position 3 in the top layer. The presence of copper is due to the grid supporting the sample, and platinum in position 2 is due to the electron beam not being perfectly confined to the very thin Al_2O_3 region.

Scan position	1	2	3
Al	1.85	23.67	0
O	11.57	34.05	0
Pt	55.28	27.4	59.78
Cu	31.27	14.86	30.31

the capacitance due to the PtO_2 is likely significantly larger than that of the ALD layer since the parasitic layer is very thin and the dielectric constant of platinum oxide can be as high as 18 if it is nonstoichiometric.[9] The observed nonlinear behavior of differential conductance can therefore be explained by considering the contribution of the PtO_2 layer in the untreated devices. The sample, as prepared and before anneal, can be modeled by a series combination of the two Al_2O_3 tunnel barriers and two parasitic PtO_2 layers. The electrical conductivity of metal oxides typically exhibits thermally activated conductance[9] and nonlinear electric field dependence[10] as was observed. Once the PtO_2 decomposes, the parasitic oxide layer turns to metal resulting in an approximately 2 orders of magnitude increase in conductance and the linear electric field response characteristic of MIM tunnel junctions.

Likewise, the behavior of the water-based devices can be explained by native PtO_2 playing a major role in satisfying Eq. (2) and poor ALD nucleation when compared to ozone with the same number of deposition cycles. For the series combination suggested above, if conductance was limited by a layer of native PtO_2 in the as prepared water-based devices, then decomposition of the PtO_2 would result in a drastic increase in conductance, as is observed, and even the breaking of Eq. (2). Furthermore, the smaller spread in conductance for ozone-based devices compared to water-based devices suggests that the ozone-based devices have a more

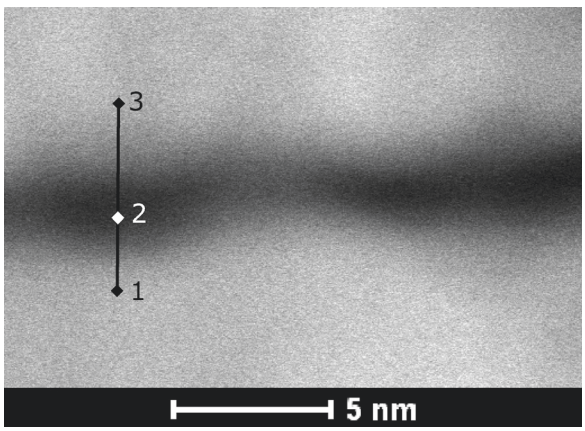

FIG. 6. Scanning TEM image showing the positions of the EDX spectra used to generate the data in Table I.

TABLE II. Atomic percentages after anneal. Positions are similar to those shown in Fig. 6 but on a different sample. Notice the decrease in oxygen content at position 1 compared to position 1 in Table I.

Scan position	1	2	3
Al	1.14	11.26	0
O	1.72	18.83	1.39
Pt	44.85	30.51	48.04
Cu	52.25	39.37	50.55

uniform ALD layer than the water-based devices. This difference in conformity is attributed to the fact that H_2O is unable to oxidize the Pt surface as O_3 is able to[11] and that the ozone-induced formation of PtO_2 promotes ALD nucleation. This theory is supported by literature about ALD on similarly inert substrates such as 2D transition metal dichalcogenides. McDonnell's study[12] of MoS_2 found that nucleation was either mediated by organic residue resulting in nonconformal ALD or depended on reactions between physisorbed precursors on the MoS_2 surface in a limited time window. Our results suggest a similar phenomenon for when H_2O is used on platinum, but that O_3 achieves more conformal ALD by oxidizing the platinum and providing a higher density of nucleation sites.

To test this theory about PtO_2, ozone-based devices were exposed to forming gas (5% H_2 in Ar) at low temperatures ($\sim$32 °C) for 1 h. According to calculations of the change in Gibbs free energy, PtO_2 should be readily reduced by the hydrogen in the forming gas even at room temperature. As was expected, the conductance increased by about a factor of 30 (0.5–15 nS). Given the lower temperature, the smaller change in conductance for this process compared to the annealing process is likely due to a much slower reaction rate and lower diffusion rate of the reaction by-products, but requires further investigation.

IV. SUMMARY AND CONCLUSIONS

Single electron transistors were fabricated with Al_2O_3 as the tunneling barrier using O_3 or H_2O as the oxygen

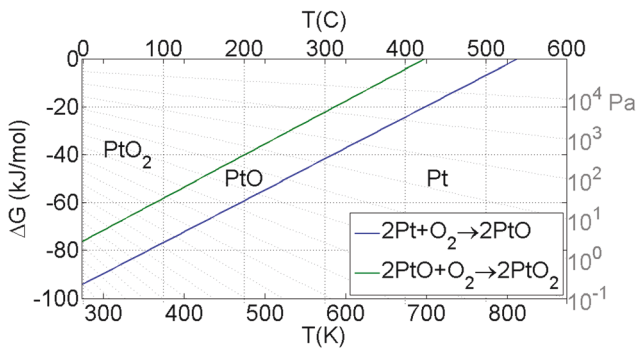

FIG. 7. (Color online) Ellingham diagram showing the change in Gibbs free energy per mole of oxygen as a function of temperature and pressure. These values were calculated using thermodynamic data from Samsonov (Ref. 11). Lower oxygen partial pressures, shown in the nomographic scale on the right, reduce the decomposition temperature by changing the $\Delta G = 0$ kJ/mol line to the lines shown in gray with the pressures indicated.

precursors. It was found that using O_3 resulted in devices with lower but more consistent and stable conductance as compared to using H_2O with the same number of cycles. It was also found that annealing increased the conductance significantly, but that annealed water-based devices were short circuits between the source and drain. TEM and EDX revealed the presence of a PtO_2 layer created during the ALD process. Given the relative instability of PtO_2, its presence provides a coherent explanation for the difference observed between annealed and untreated devices, and suggests that the oxidation of Pt by O_3 causes more uniform ALD growth and hence better device repeatability. Adding credence to this theory is the fact that devices exposed to hydrogen-containing forming gas experienced a smaller but still significant increase in conductance. Future work will investigate possible advantages and disadvantages of high temperature annealing versus low temperature reduction in forming gas, and whether exposures to forming gas or even pure hydrogen can result in increases in conductance of a similar magnitude to those observed with annealing.

This work also shows that for ALD on metals, there is a delicate tradeoff between facilitating ALD nucleation and oxidizing the metal substrate: a stronger oxidizing agent or more reactive metal may provide better nucleation but it also oxidizes deeper into the metal. Platinum and ozone provide a nice balance between these two objectives since ozone is reactive enough to oxidize platinum and provide better nucleation, but platinum's oxide is unstable enough that it can be easily reduced or even decomposed. This may prove important as devices that exploit tunneling such as SETs and tunnel FETs become more prevalent.

ACKNOWLEDGMENTS

The authors would like to acknowledge the National Science Foundation (NSF DMR-1207394) for funding. Special thanks to the Notre Dame Nanofabrication Facility (NDNF) for advice in the fabrication process and to the Notre Dame Integrated Imaging Facility (NDIIF) for acquisition of the TEM and EDX data.

[1]K. K. Likharev, Proc. IEEE **87**, 606 (1999).
[2]T. A. Fulton and G. J. Dolan, Phys. Rev. Lett. **59**, 109 (1987).
[3]G. Pardon, H. K. Gatty, G. Stemme, W. van der Wijngaart, and N. Roxhed, Nanotechnology **24**, 015602 (2013).
[4]R. Kuse, M. Kundu, T. Yasuda, N. Miyata, and A. Toriumi, J. Appl. Phys. **94**, 6411 (2003).
[5]M. Pierre, M. Hofheinz, X. Jehl, M. Sanquer, G. Molas, M. Vinet, and S. Deleonibus, Eur. Phys. J. B **70**, 475 (2009).
[6]M. P. Herrero Fernandez and B. L. Chamberland, J. Less Common Metals **99**, 99 (1984).
[7]D. Friebel *et al.*, Phys. Chem. Chem. Phys. **13**, 262 (2011).
[8]H. J. T. Ellingham, J. Soc. Chem. Ind. **63**, 125 (1944).
[9]H. Neff, S. Henkel, E. Hartmannsgruber, E. Steinbeiss, W. Michalke, K. Steenbeck, and H. G. Schmidt, J. Appl. Phys. **79**, 7672 (1996).
[10]L. M. Levinson and H. R. Philip, J. Appl. Phys. **46**, 1332 (1975).
[11]*The Oxide Handbook*, edited by G. V. Samsonov, translated by C. N. Turton and T. I. Turton (Plenum, New York, 1973).
[12]S. McDonnell *et al.*, ACS Nano **7**, 10354 (2013).